Supplement of Earth Syst. Sci. Data, 15, 3623–3639, 2023
https://doi.org/10.5194/essd-15-3623-2023-supplement

Open Access Earth System Science Data

Supplement of

Global urban fractional changes at a 1 km resolution throughout 2100 under eight scenarios of Shared Socioeconomic Pathways (SSPs) and Representative Concentration Pathways (RCPs)

Wanru He et al.

Correspondence to: Xuecao Li (xuecaoli@cau.edu.cn) and Yuyu Zhou (yuyuzhou@hku.hk)

Supplementary texts

The Logistic-Trend-ISA-CA model is a self-evolution system, consisting of four primary components, including the suitability surface (here we implemented a logistic regression model for transition rules extraction, Eq. S1-2), the trend-adjusted neighborhood (Eq. 2-3), the stochastic perturbation (Eq. S3), and the land constraint.

We implemented a logistic regression model for transition rules extraction with considerations of various spatial proxies. Specifically, we identified those changed and persistent pixels with ISA increment threshold of 0.5 and collected these two sample groups using the stratified sampling strategy (i.e., with a sample rate of 20%). Thereafter, the suitability surface was derived using the regression model based on those spatial proxies, including the DEM, slope (calculated from DEM), minimum distance to city centers, minimum distance to different grades of roads, as well as various land covers (i.e., evergreen needleleaf forests, evergreen broadleaf forests, deciduous needleleaf forests, deciduous broadleaf forests, mixed forests, open shrublands, savannas, grasslands, permanent wetlands, croplands, cropland/natural vegetation mosaics, urban and built-up lands, permanent snow and ice, barren, water bodies). The neighborhood configuration, which closely relates to its size, shape, and surrounding land cover types, is a basic and crucial component in the urban CA model as a driving force to modeling urban dynamics. Most urbanized pixels were developed following the historical pathway coupling with the neighborhood altering by the temporal trend. In this procedure, the non-urban grids are more likely to transform into urban grids in next iterations if there are more developed urban grids surrounded. Thereafter, the weighting factors of urban pixels developed in more recent years are higher than those developed in earlier years. We also included land constraint and stochastic perturbation in the developed Logistic-Trend-CA model. Land cover/use type in the initial year will influence spatial allocation in the urban sprawl process and restricted lands, such as water and protected areas, were not allowed for development in the Logistic-Trend-CA model; thereafter, they were represented as a land constraint term as Land = 0. Stochastic perturbation represents unconsidered factors (e.g., policies) in the modeling process.

$$z = b_0 + b_1 x_1 + \ldots + b_n x_n \tag{S1}$$

$$p_{suit} = \frac{\exp(z)}{1+\exp(z)} \tag{S2}$$

$$SP = 1 + (-\ln(\varphi))^{\alpha} \tag{S3}$$

where P_{suit} is the obtained suitability of development from the biophysical and socioeconomic conditions and b_i and x_i are the ith coefficient and spatial proxy, respectively. Ω is the influence of neighborhood considering the historical contexts of urban sprawl using a weighting factor of W_{ij}^{ts} (Eq. 2-3). SP is the stochastic perturbation, φ is a random value in [0, 1], and α is a parameter determining the degree of perturbation.

We then calculated the overall development probability based on the suitability surface, neighborhood, land constraint and stochastic perturbation. We determined their development probabilities P_{suit} using

Eq. (4) based on urban time series data derived from Landsat. The units with the higher combined development probability have higher priority for urban grid allocation than those with lower probability.

Fig. S1

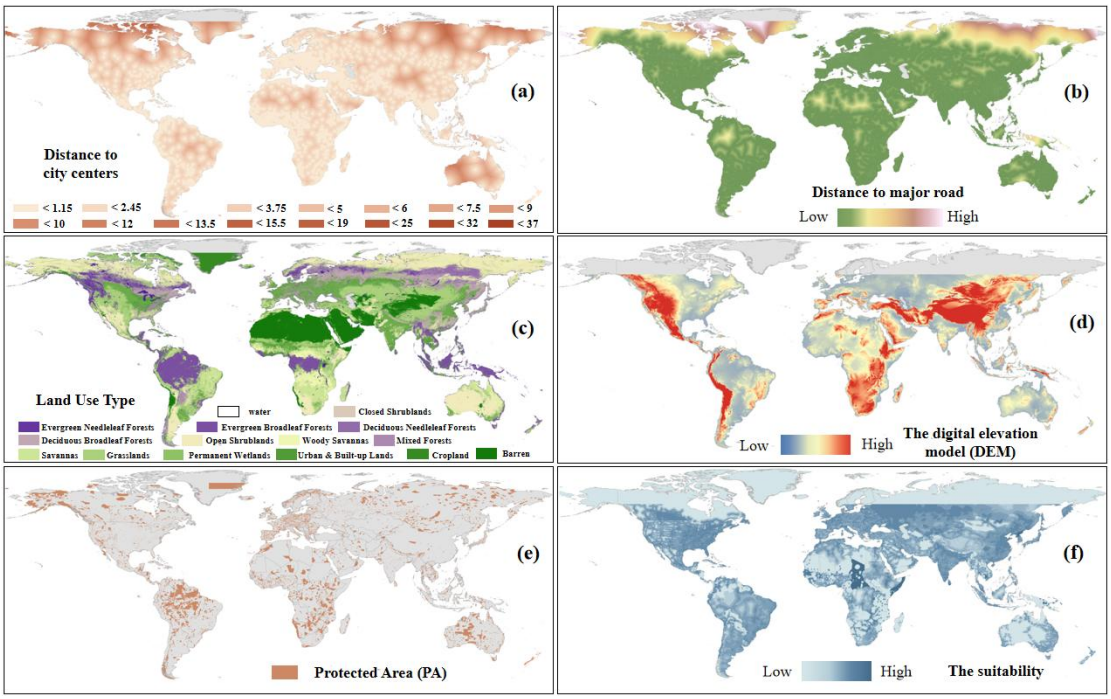

Fig. S1. The distance to city centers (a), the distance to major road (b), the land use types (c), the digital elevation model (DEM) (d), the protected area (PA) (e), and the derived suitability surface at the global scale (f)

Fig. S2

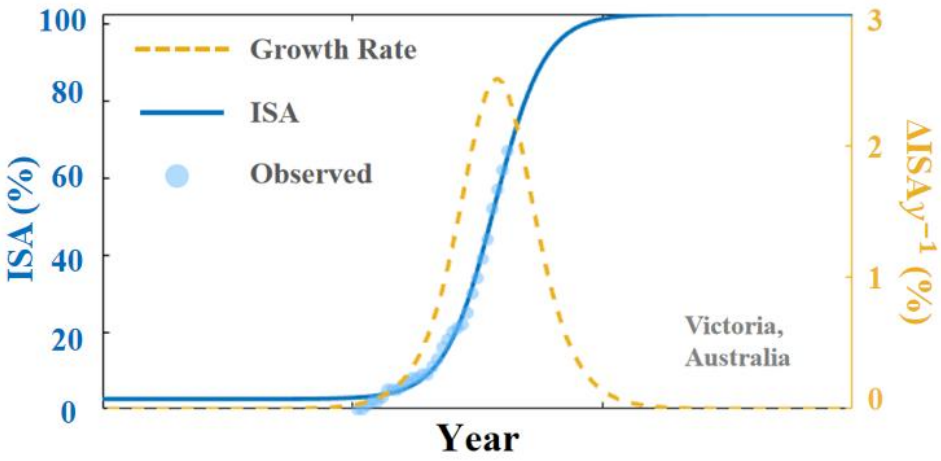

Fig. S2. Illustration of the ISA-based urban area growth model in a specific region, with distinct ISA growth trends at different urbanization levels. Here we set the ISA conceptual model of Victoria in Australia as an example.

Fig. S3

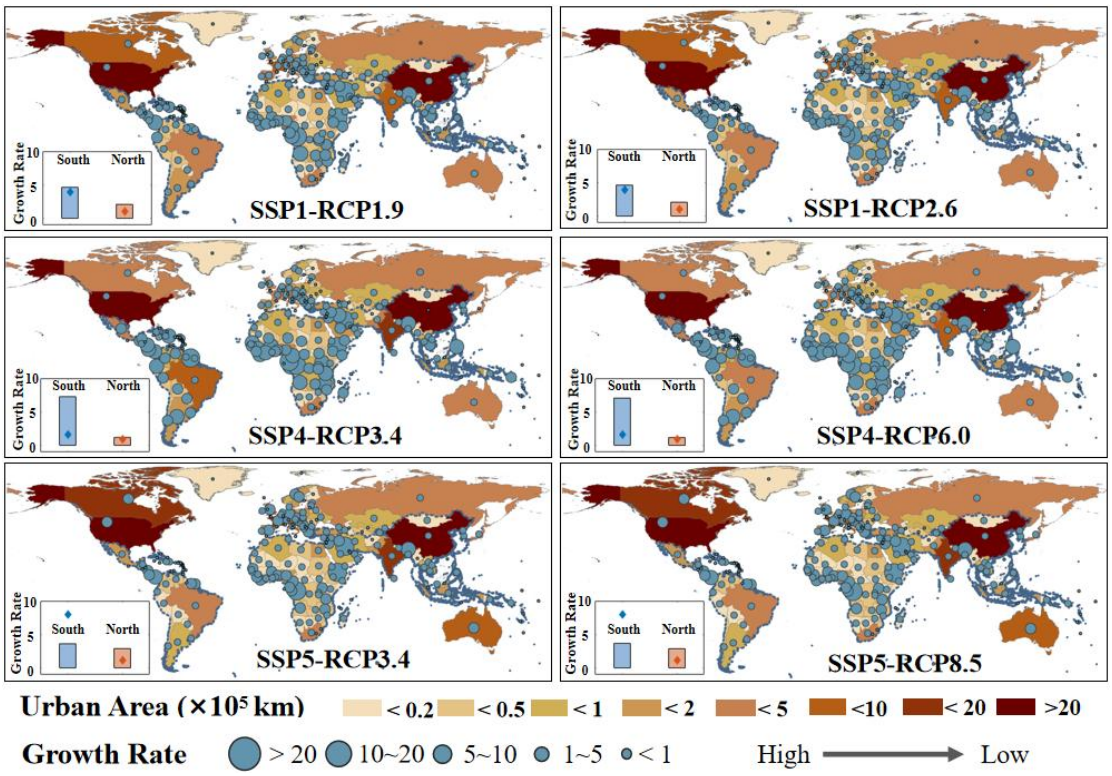

Fig. S3. The average urban growth rate (2100/ 2015) derived from LUH2 at the country level, under various RCP levels and same SSP levels.

Fig. S4

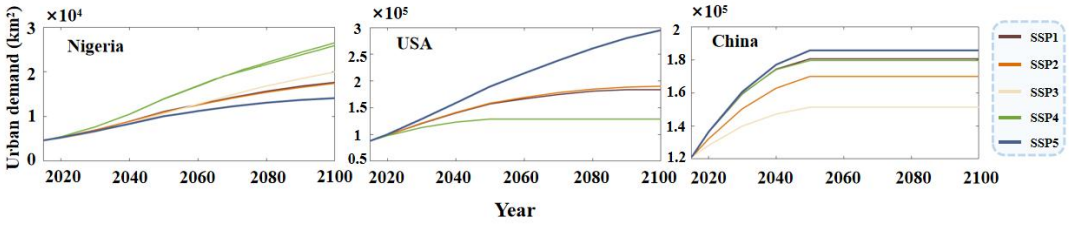

Fig. S4. The future urban demand of the typical countries in Fig. 3.

Fig. S5

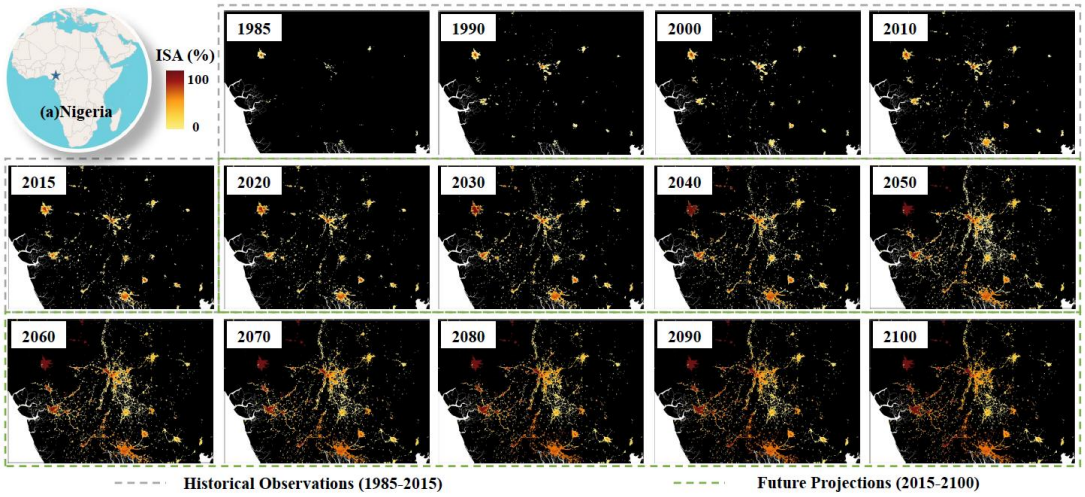

Fig. S5. The temporal spatial patterns of urban sprawl of Nigeria at 1km spatial resolution from 1985 to 2100 under the most fluctuating scenario (SSP4-RCP6.0).

Fig. S6

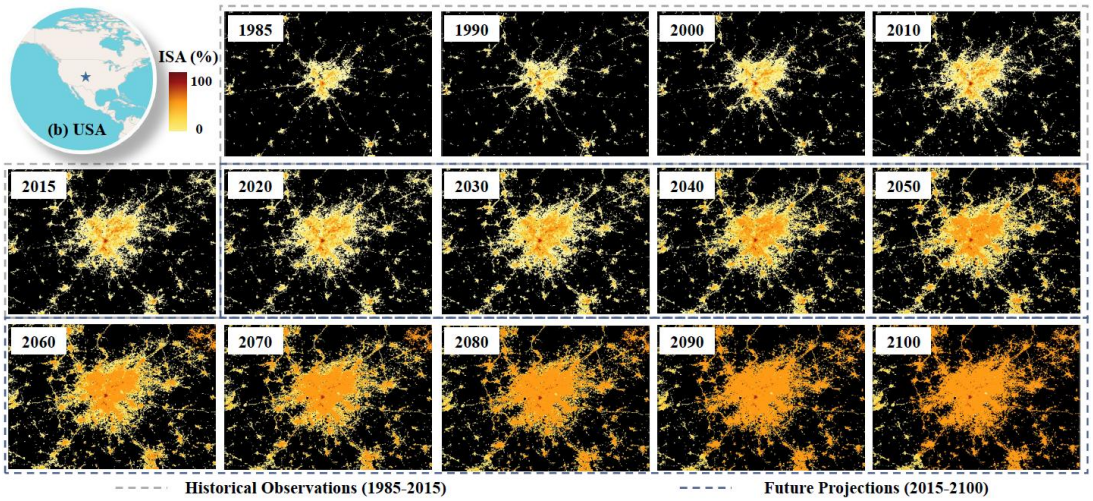

Fig. S6. The temporal spatial patterns of urban sprawl of USA at 1km spatial resolution from 1985 to 2100 under the most fluctuating scenario (SSP5-RCP8.5).

Fig. S7

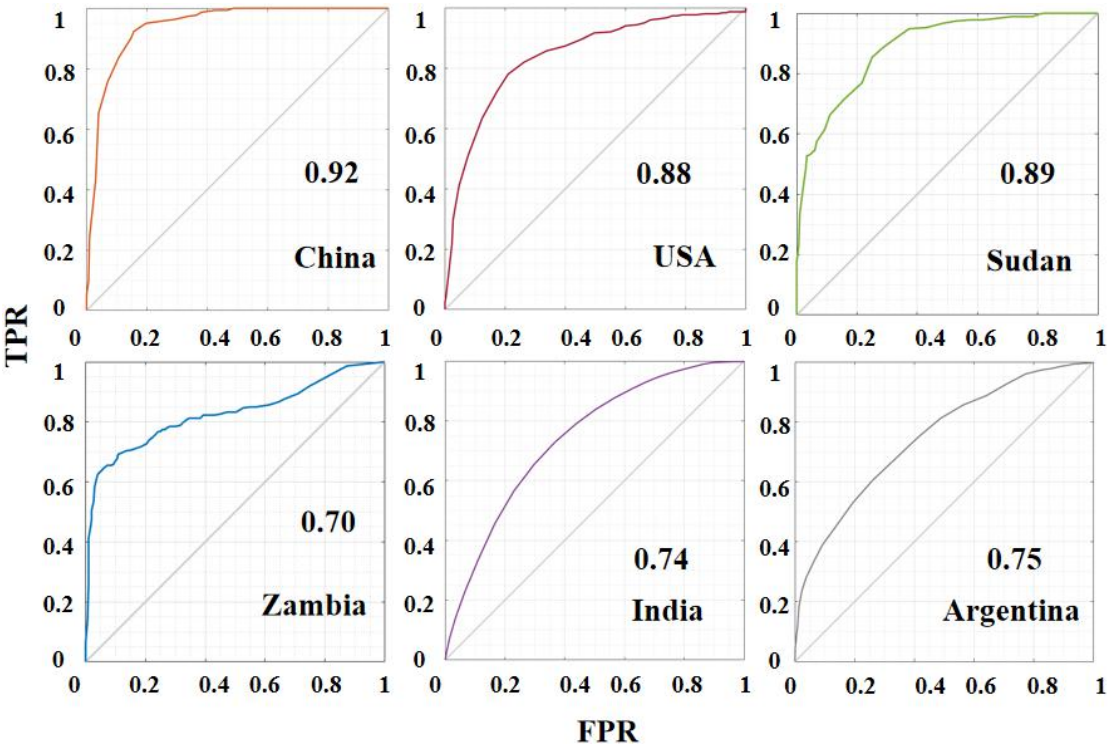

Fig. S7. The ROC curves in some representative countries like China, USA, Sudan, Zambia, India, and Argentina.

Fig. S8

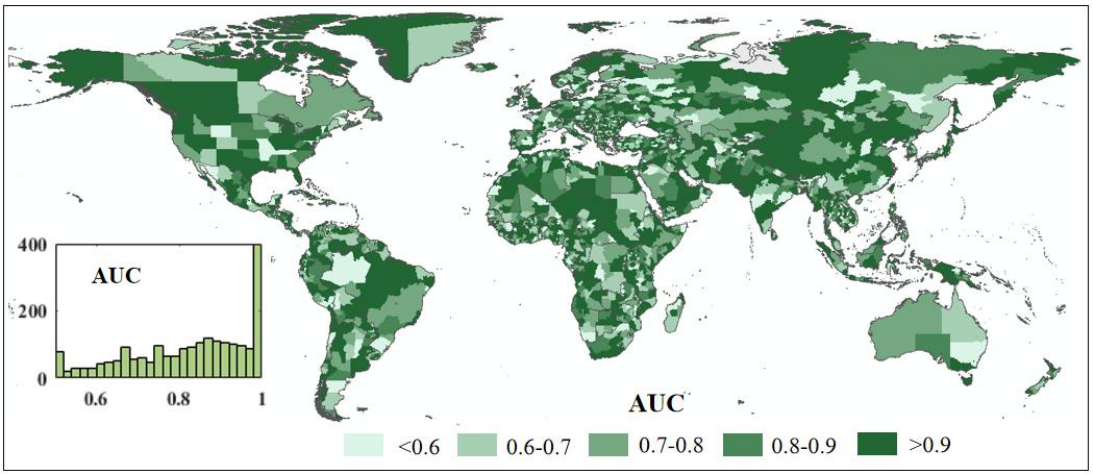

Fig. S8. The model performance of derived suitability surfaces at the state-level using the indicator of the area under the curve (AUC) at the global scale.

Fig. S9

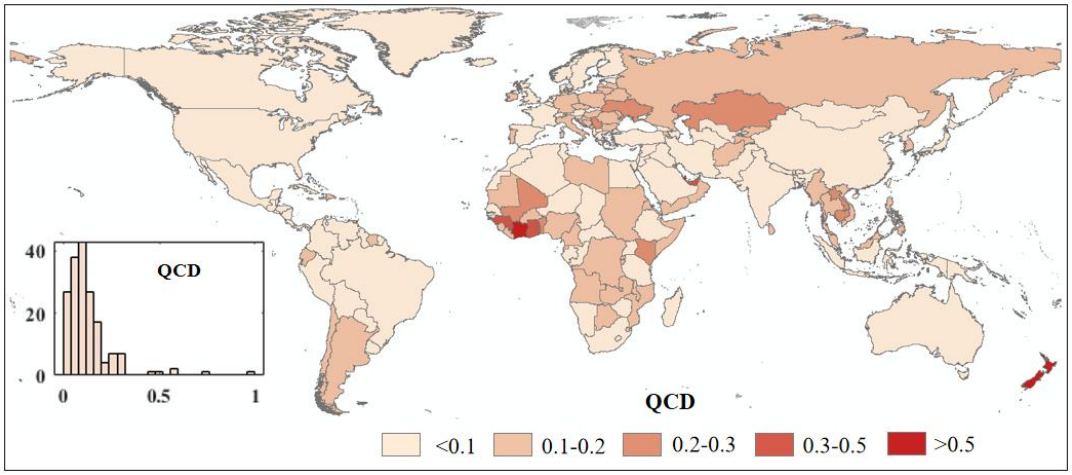

Fig. S9. The quartile coefficient of dispersion (QCD) within each country at the global scale during the overlap period (1990-2015).

Fig. S10

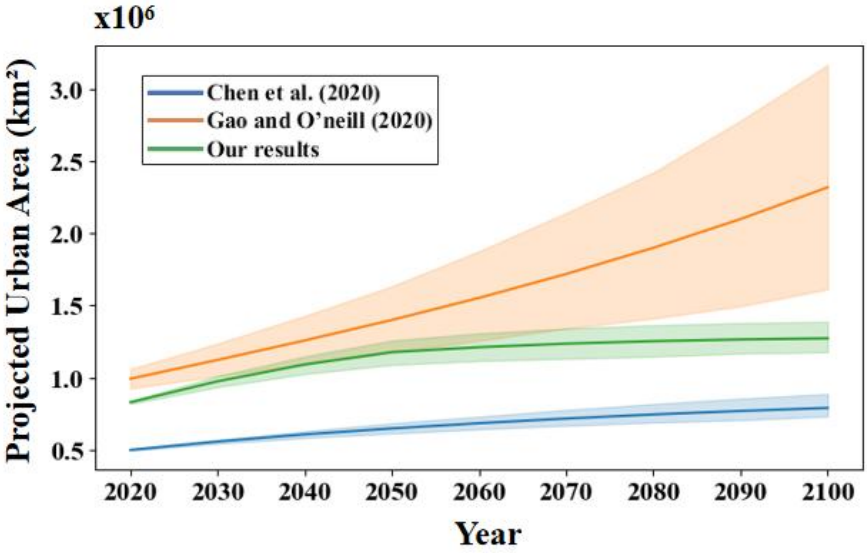

Fig. S10. The projected urban area of our results with two similar global urban datasets from Gao and O'neill (2020) and Chen et al. (2020a) under all future scenarios across years.